

SEGMENTATION OF MALARIA PARASITES IN PERIPHERAL BLOOD SMEAR IMAGES

Vishnu V. Makkapati

Philips Research Asia - Bangalore
Philips Electronics India Limited
Bangalore - 560 045, Karnataka, India
Email: vishnu.makkapati@philips.com

Raghuveer M. Rao

Department of Electrical Engineering
Rochester Institute of Technology
Rochester, NY 14623-5603
Email: mrreee@rit.edu

ABSTRACT

Detection of malaria parasites in stained blood smears is critical for treatment of the disease. Automation of this process will help in reducing the time taken for diagnosis and the chance for human errors. However, the variability and artifacts in microscope images of blood samples pose significant challenges for accurate detection. A scheme based on HSV color space that segments Red Blood Cells and parasites by detecting dominant hue range and by calculating optimal saturation thresholds is presented in this paper. Methods that are less computation-intensive than existing approaches are proposed to remove artifacts. The scheme is evaluated using images taken from Leishman-stained blood smears. Sensitivity and specificity of the scheme are found to be 83% and 98% respectively.

Index Terms— Segmentation, malaria diagnosis, chromatin dot detection

1. INTRODUCTION

Malaria is a widely prevalent disease affecting millions of people in various parts of the world. Microscopic observation of blood smears of patients is considered the *gold standard* of diagnosis. The blood smears are usually observed by a person manually and the quality of diagnosis is thus dependent on the level of training of the observer. Further, the time taken to observe a smear typically ranges between 15-20 minutes. Automatic processing of the blood smear images will help in providing fast and consistent diagnosis. This paper deals with results of investigation into the development of image processing schemes for this purpose.

There are examples of work on diagnosis of malaria from blood smear images in the literature. The method in [1] transforms the images to match the characteristics of a reference color image. A Bayesian pixel classifier is used to mark stained pixels and features are extracted from them. A distance weighted K-nearest neighbor classifier is trained with them to classify the pixels as parasite and non-parasite. The method proposed in [2] attempts to mimic a human technician. It uses morphological and threshold selection

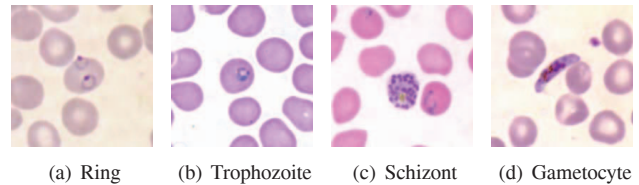


Fig. 1. *P. falciparum*: Stages found in blood [4]

techniques to identify (red blood cells) RBCs and parasites. Image features based on color, texture and geometry of RBCs and parasites are generated. These are presented to a two-stage tree classifier using back-propagation feed-forward neural networks for species classification. The scheme discussed in [3] is based on a multi-stage estimation process with minimal prior knowledge starting from a representation of RBCs. It compensates for imaging variability by using a correction process on the intensity component in HSI space. An elliptic template is designed and used to extract RBCs from an image.

In this paper we present techniques to segment parasites in stained images. The scheme is based on segmentation of RBCs and parasites in HSV color space and handles the variability of the images. Distinguishing features of this work are: (a) Focus on segmentation/detection of chromatin dots for malaria diagnosis whereas earlier approaches focused on gross level features extracted from RBCs without looking at parasite components (b) Incorporation of accuracy enhancing features such as geometric distance measurement for false positive reduction (c) Handling of image variability without need of normalizing with respect to a standard (d) Adaptation of parameters to a given image without need to train and (e) Use of Leishman-stained images which are widely used in malaria infested rural areas of India.

2. BACKGROUND

P. falciparum, *P. vivax*, *P. ovale*, and *P. malariae* (*P.* for plasmodium) are the four species of malaria that infect human



Fig. 2. Hue scale [5]

Table 1. Hue angle and color type

Hue Angle	Color Type
0°	red
60°	yellow
120°	green
180°	cyan
240°	blue
300°	magenta

beings. The parasite appears in four stages in blood - ring, trophozoite, schizont, and gametocyte. These stages are identified based on the appearance of cytoplasm and chromatin dots. They take different forms depending on the species and stage of the parasite (Fig. 1). The chromatin dots are the dotted structures seen in all four subfigures. They are the DNA complex of the parasite. A lot of them are seen in the schizont and gametocyte stages while one or two are seen in the ring stage. The purplish material (including the rings in Fig. 1(a)) is the cytoplasm within the parasite.

The malaria parasites infect RBCs and hence are usually located inside them. Pathologists use color as a cue to identify RBCs and parasites in stained samples viewed with a microscope. However, segmenting RBCs and parasites in an image is not a trivial task. This is because of the fact that the colors of the background, RBCs and parasites vary depending on the pH of the buffer used for smear preparation as shown in Fig. 1. Further, the presence of artifacts (objects other than RBCs and parasites) complicates the segmentation process.

3. PROPOSED SCHEME

We segment the RBCs and then check if a parasite(s) has infected them. We develop a color-based method to segment parasites and RBCs. Chromatin dots are more easily distinguished from the RBC than cytoplasm which is a delicate structure that shows great variability. Hence our approach focuses on isolating chromatin dots in the image. The input images are obtained in RGB color space. Since the RGB color space is not intuitive for processing, we choose the HSV color space which offers a convenient representation where hue, saturation, and value indicate the quality by which we distinguish one color family from another, a strong color from a weak one, and a light color from a dark one respectively [5]. Figure 2 and Table 1 show the hue angles and the corresponding color types.

We choose appropriate ranges of hue and saturation to segment RBCs and chromatin dots. However, the same hue

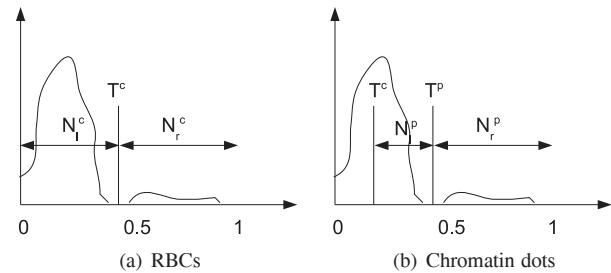


Fig. 3. Schematic illustrating the calculation of optimal thresholds to segment RBCs and chromatin dots from saturation histogram.

and saturation values cannot be used for all images due to color variability (Fig. 1) and hence have to be adaptively chosen for each input image. One approach to overcome color variability would be to transform each input image to a nominal reference color distribution [1]. However, there is enough variability between the objects of interest (RBCs and parasites) and the background that even with such a transformation, there is no assurance that such objects occupy well defined color ranges in the final image. We therefore propose an approach where we dynamically determine the background and process the remaining pixels to identify the objects.

The dominant color in these images is representative of the background (i.e., region excluding RBCs and parasites). We divide the entire hue range of 360° into six segments where each segment has a width of 60° and is centered around a color type as given in Table 1. Then we determine the dominant color type p by finding the number of pixels N_i that fall within each hue segment i , $1 \leq i \leq 6$ and identifying the peak value N_p (i.e. p is associated with the mode of the hue distribution). The pixels corresponding to the remaining segments i , $1 \leq i \leq 6$ and $i \neq p$ are segmented to identify RBCs and chromatin dots by using an appropriate saturation threshold. However, if the dominant color type exceeds a certain l percentage of the total pixels (i.e., $\frac{N_p}{\sum_{i=1}^6 N_i} > l\%$), then only the saturation component is used for segmentation.

Optimal saturation thresholds to segment RBCs and chromatin dots have to be identified. We use the method proposed in [6] to select an optimal saturation threshold to segment RBCs. The method was found to give an optimal threshold for bimodal distributions but did not work well for unimodal distributions such as the one shown in Fig. 3(a). To overcome this problem we use the fact that RBCs typically occupy a certain percentage of the area of an image. We count the number of pixels N_r^c and N_l^c respectively that exceed and fall below the specified threshold T^c (Fig. 3(a)). If $\frac{N_r^c}{N_l^c} > n\%$ for some n (our measurements with the images show this to 10%), then the threshold T^c is valid. Otherwise we derive the threshold by applying Otsu's method to the pixels that fall below this threshold. The process is repeated until convergence.

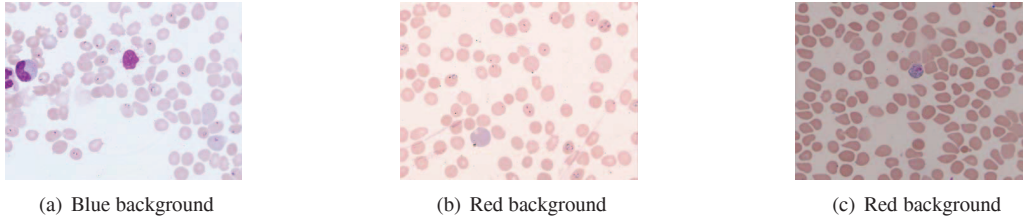


Fig. 5. Sample images of *P. Falciparum*

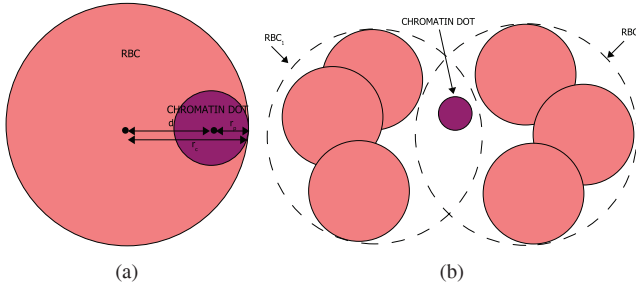


Fig. 4. (a) Schematic showing the containment of chromatin dot in RBC. The bold dots indicate the centroids of RBC and chromatin dot. d , r_c and r_p denote the distance between centroids, radius of RBC and radius of chromatin dot respectively. (b) Schematic showing the false containment of chromatin dot in RBC.

The saturation values of the chromatin dots fall in the outlier zone of the histogram. To segment chromatin dots we make use of the fact that parasite pixels occupy at most a certain fraction of the RBC pixels (considering the maximum parasite density possible). Figure 3(b) shows a schematic for computing the threshold to segment chromatin dots. Only those pixels that belong to the RBCs are processed. If $\frac{N_p^p}{N_p^r} < m\%$ for some m (typically 2%), then the threshold T^p is considered valid. Otherwise we apply the threshold selection method again to the pixels that fall above this threshold. The process is again repeated until convergence.

The segmented images are often found to contain noise and the RBCs are found to have holes (vacuoles) inside. We overcome these problems to a certain extent by using morphological filtering with a circular structuring element of radius 3. The filtered images are labeled to assign unique numbers to chromatin dots and RBCs. The platelets typically pass the thresholds set for RBC segmentation. However, the area of a platelet is much smaller compared to that of an RBC and an area threshold is used to eliminate them. Further, the artifacts and nuclei of White Blood Cells (WBCs) tend to pass the thresholds for chromatin dots. The areas of nuclei of WBCs are larger as compared to that of a chromatin dot and hence an appropriate threshold is used to remove them.

To remove the other artifacts, we use the fact that parasites



Fig. 6. Hue and saturation histograms for image in Fig. 5(a)

are usually located in RBCs. To detect whether a chromatin dot is within an RBC we propose a two-step method. We compute the centroids for each RBC i and each chromatin dot j denoted by (x_c^i, y_c^i) and (x_p^j, y_p^j) respectively. We then determine the radius of the Minimum Bounding Circle (MBC) of each RBC (r_c^i) and each chromatin dot (r_p^j). A chromatin dot j is present within RBC i if

$$\sqrt{(x_c^i - x_p^j)^2 + (y_c^i - y_p^j)^2} \leq r_c^i + r_p^j \quad (1)$$

This is schematically represented in Fig. 4(a). However, this scheme may not yield appropriate results if the RBCs overlap each other as illustrated in Fig. 4(b). To overcome this problem, we check if the number of overlapping chromatin dot and RBC pixels exceed a certain percentage (say $k\%$) of the area of a chromatin dot. Classification as chromatin dot is declared to be valid if this condition is satisfied.

4. EXPERIMENTAL RESULTS

We have evaluated the performance of our scheme using several images taken from Leishman-stained blood smears. The resolution of the images considered is 1391×1040 and with 8 bits per color component. The images are median filtered using a window of size 3×3 to remove noise.

Figure 5 shows three of the images used in our experiments. The hue histogram for the image in Fig. 5(a) is shown in Fig. 6(a). The number of pixels in each hue segment for the images in Fig. 5 are given in Table 2. The algorithm identifies blue as the background color for the image in Fig. 5(a) and red for the images in Fig. 5(b) and Fig. 5(c) respectively. These are consistent with visual observation as well.

The saturation histogram for the image in Fig. 5(a) is shown in Fig. 6(b). For this image the method proposed in [6] has resulted in an incorrect threshold value of 0.3255

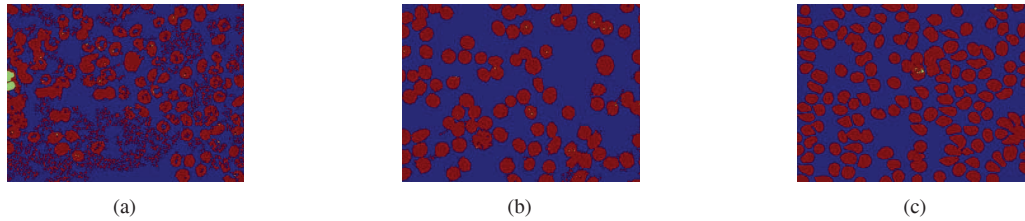


Fig. 8. Segmented images for the images in Fig. 5 where blue, red and green colors indicate the pixels corresponding to background, RBCs and chromatin dots respectively.

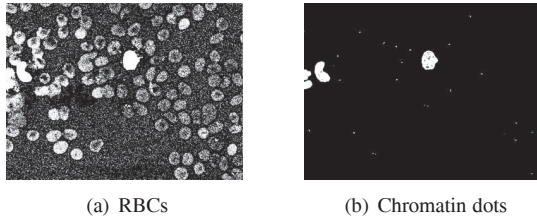


Fig. 7. Initial segmentation of the image in Fig. 5(a)

Table 2. No. of pixels in each hue segment

Color Type	Fig. 5(a)	Fig. 5(b)	Fig. 5(c)
red	39224	1326997	1351771
yellow	565	104424	35036
green	1356	292	51
cyan	253361	122	28
blue	717312	108	2232
magenta	435862	15737	58562

to segment RBCs. The adaptive threshold selection scheme (Fig. 3(a)) has resulted in a threshold value of 0.0863 which is found to be the right choice. Repeated experiments have revealed that a saturation threshold value of 0.4 is optimal to segment chromatin dots (Fig. 3(b)). The RBC and chromatin dot images obtained after initial hue and saturation segmentation are shown in Fig. 7(a) and Fig. 7(b). However, these images contain noise and many artifacts which are eliminated to a great extent by using the methods presented in Sec. 3. The final segmented images are shown in Fig. 8. Evaluation of the scheme with 55 annotated images showed that the sensitivity and specificity of the scheme are 83% and 98% respectively.

5. CONCLUSIONS

A method to segment RBCs and chromatin dots in images taken from Lishman-stained blood smears is presented. The method operates in HSV space and is dynamic in the sense that relevant thresholds are determined from the statistics of the given image rather than keeping them fixed for all images. The performance of the scheme was evaluated using

images with color variability. The background in an image is determined using the dominant hue range. The remaining pixels are processed to segment RBCs and chromatin dots. Schemes are proposed to determine optimal saturation thresholds to segment RBCs and chromatin dots that are robust with respect to the color variability encountered. The work illustrates the potential of color image processing techniques in providing diagnostic solutions to serious infections afflicting a significant portion of the world's human population and are being pursued for the development of low cost portable testing kits.

6. ACKNOWLEDGEMENTS

The authors would like to thank clinical partners Prof. Raviraj V. Acharya and Dr. Chethan Manohar of Kasturba Medical College, Manipal University, India for providing the data.

7. REFERENCES

- [1] F. B. Tek, A. G. Dempster, and I. Kale, "Malaria parasite detection in peripheral blood images," in *Proc. British Machine Vision Conference*, Edinburgh, September 2006.
- [2] N.E. Ross, C.J. Pritchard, D.M. Rubin, and A.G. Dus, "Automated image processing method for the diagnosis and classification of malaria on thin blood smears," *Medical and Biological Engineering and Computing*, vol. 44, no. 5, pp. 427 – 436, May 2006.
- [3] S. Halim, T. Bretschneider, Y. Li, P. Preiser, and C. Kuss, "Estimating malaria parasitaemia from blood smear images," in *Proc. ICCARV. IEEE*, 2006, pp. 648 – 653.
- [4] "CDC DPDx - malaria image library," http://www.dpd.cdc.gov/DPDx/HTML/ImageLibrary/Malaria_il.htm.
- [5] A.H. Munsell, *A Color Notation*, Munsell Color Corporation, Baltimore, MD, 1946.
- [6] N. Otsu, "A threshold selection method from gray-level histograms," *IEEE Trans. Syst., Man, Cybern.*, vol. 9, no. 1, pp. 62 – 66, 1979.